Pulsed NMR: Determinations of γ and the Use of Spin-Echo Techniques for Measuring Relaxation Times

Edwin Ng*
MIT Department of Physics
(Dated: November 16, 2011)

Using pulsed NMR, we determine the gyromagnetic ratios of ^{1}H and ^{19}Fl nuclei, and utilize spin echoes for measuring the spin-spin relaxation time for aqueous glycerin solutions and the spin-lattice relaxation time for solutions of Fe^{3+}. We find $\gamma = (2.728 \pm 0.016) \times 10^8\,\mathrm{s^{-1}T^{-1}}$ for ^{1}H and $\gamma = (2.570 \pm 0.015) \times 10^8\,\mathrm{s^{-1}T^{-1}}$ for ^{19}Fl. We examine the dependence of the respective relaxation times on glycerin viscosity and ion concentration, and confirm N. Bloembergen's inverse linear relationship between spin-spin relaxation time and viscosity in log-log space.[1]

I. THE THEORY OF NMR

Nuclear magnetic resonance (NMR) is a method for exploring the structure of materials by measuring the effects of perturbing their internal magnetic dipoles, pioneered by Felix Bloch and Edward Purcell in the 1940s. The following discussion draws from [2].

Classically, the magnetic moment $\boldsymbol{\mu}$ of a charged rigid body is related to its angular momentum $\mathbf{S}$ by $\boldsymbol{\mu} = \gamma\mathbf{S}$, where γ is the gyromagnetic ratio. In a uniform magnetic field $\mathbf{B_0}$, $\boldsymbol{\mu}$ gyroscopically precesses about of $\mathbf{B_0}$ with the Larmor frequency

$$\omega_0 = \gamma B_0. \tag{1}$$

In quantum mechanics, atomic nuclei with an odd number of nucleons possess an intrinsic spin angular momentum and hence also a magnetic moment and gyromagnetic ratio γ. Although the spin state of a single nucleus is non-classical, Bloch showed that for an ensemble of spins, the average magnetization $\mathbf{M}$ of the sample (viz. the expectation of the sum of the nuclear magnetic moments) obeys classical laws. Thus, when the sample is placed in a field $\mathbf{B_0}$, $\mathbf{M}$ will, like $\boldsymbol{\mu}$, exhibit Larmor precession according to Equation 1

In pulsed NMR, the sample is placed in a large magnetic field $\mathbf{B_0} = B_0\hat{\mathbf{z}}$ and a probe pulses the sample with a perturbing radio frequency (RF) signal. The RF pulse produces an alternating magnetic field $\mathbf{B_1}$ along $\hat{\mathbf{x}}$, with $B_1 \ll B_0$. When the frequency of the RF signal is close to the Larmor frequency ω_0, the effect of the pulse is to cause a secondary, slow precession of $\mathbf{M}$ about $\hat{\mathbf{y}}$. The rate of the slow precession is $\gamma B_1/2$, so an RF signal near ω_0 with duration $\pi/(\gamma B_1)$ is called a 90° pulse—it rotates a $\mathbf{M}$ initially aligned with $\hat{\mathbf{z}}$ into the transverse xy-plane. After the 90° pulse, the spin rotates in the xy-plane due to Larmor precession. Similarly, a pulse with twice this duration is a 180° pulse and flips $\mathbf{M}$.

Because of the ensemble nature of $\mathbf{M}$, the application of RF pulses perturbs the system away from equilibrium. At the end of a 90° pulse, two effects are of interest.

The first is the return to thermal equilibrium as $\mathbf{M}$ regains its longitudinal magnetization along $\hat{\mathbf{z}}$. The return is exponential, characterized by a decay time called the spin-lattice relaxation time T_1. Longitudinal remagnetization is caused by interaction of the nuclei with their environment (the lattice) and the resulting dissipation of the absorbed RF energy. For example, the presence of paramagnetic ions in a sample strongly decreases T_1 by introducing microscopic magnetic fields that disperse the energy absorbed by the spins in the RF pulse.[3] This lab will use Fe^{3+} in studying such an effect.

The other effect is the loss of phase coherence in the xy-plane, resulting in the exponential decrease of the transverse magnetization, characterized by a time constant T_2^*. The dominant contribution to the decay is nonuniformity in $\mathbf{B_0}$, causing nuclei in different parts of the sample to precess at different rates. However, the more interesting effect comes from spin-spin interactions among the nuclei. We can write

$$1/T_2^* = 1/T_2 + \gamma\Delta H_0$$

where ΔH_0 measures the inhomogeneity of $\mathbf{B_0}$. Here, T_2 is the spin-spin relaxation time, which characterizes the interactions among the spins of the sample. These interactions cause the phases of the spins to decohere irreversibly, leading to a decay of the transverse magnetization. We explore in the effects of viscosity on spin-spin relaxation in this lab.

To eliminate the dominant effect of the field inhomogeneity, we use the phenomenon of spin echoes discovered by Erwin Hanh.[4] At a time τ after the 90° pulse, we apply a 180° pulse, which reverses the direction of precession for each part of the sample, so that at time 2τ, the transverse magnetization refocuses, leading to a *spin echo*. The decay in the spin echo amplitude as a function of τ is thus a direct measure of the decoherence due to spin-spin relaxation, bypassing the field inhomogeneity.

II. EXPERIMENTAL SETUP

The following brief summary of the experimental setup follows that given in [2], which also contains a labelled photograph of the components mentioned below.

* ngedwin@mit.edu

The NMR samples are contained in sealed 10 mm test tubes and inserted into a ten-turn coil of #18 copper wire. The sample is placed along the $\hat{\mathbf{x}}$ direction between two large permanent magnets with a field strength of approximately 1700 G, directed along $\hat{\mathbf{z}}$. In addition to sending an RF pulse to the sample, the probe picks up the induced emf due to rotation of $\mathbf{M}$ in the xy-plane. The probe circuit itself contains a tunable capacitor we can adjust to supply efficient power to the sample and is impedance matched to 50 Ω at resonance.

There are three parts to the logic of the experimental setup. First, the RF signal is output by a function generator and sent to the probe circuit, which delivers the pulse to the sample. However, in order to effect 90° and 180° pulses, the signal is also gated by a digital pulse programmer, which controls the timing of each RF pulse. Finally, the induced emf picked up by the probe is combined with the output of the function generator using a phase detector and sent to an oscilloscope.

The RF signal is generated by an Agilent 15 MHz frequency synthesizer outputting sine waves of amplitudes around 1–2 V at 10 dBm. A 3 dB power splitter sends the output to the probe circuit and the phase detector. The former is gated by a double-balanced mixer controlled by TTL pulses output by the pulse programmer. After the gate, the pulse is sent through a 33 dBm power amplifier capable of 2 W output and into the probe circuit.

The detected emf from the sample's magnetization goes into a Tron-Tech preamp and through a band pass filter at 7.5 MHz. The output is sent into a Mini-Circuits phase detector, which mixes the signal with the original RF signal from the function generator, and outputs the result to the oscilloscope.

Finally, the digital pulse programmer is a simple interface on which we can set two pulse widths PW1 and PW2 (units of 1 µs), a time delay τ between the pulses (units of 1 ms), and the repeat time between each pulse sequence (units of 10 ms). We use these pulse widths to set the 90° and 180° pulses.

The pulse programmer is capable of generating a number of sequences: (1) a single sequence of PW1 – τ – PW2; (2) a repeated sequence of PW1 – τ – PW2; (3) a series corresponding to the Carr-Purcell method, and finally; (4) a PW2 – τ – PW1 – PW2 sequence for the "Three Pulse" inversion recovery method. Of these, we are primarily interested in the second and fourth, whose utilities will be discussed in Section III. The pulse programmer is also responsible for sending a trigger signal to the scope.

The oscilloscope monitors the output of the phase detector, with typical values on the order of ~ 10 mV. A sample oscilloscope trace is shown in Figure 1, for a 90° – τ – 180° sequence; it shows most of the salient features of a phase detector signal when the RF frequency ω is near (but off) resonance, $\omega \approx \omega_0$. The amplitude of the signal is proportional to the net transverse magnetization. The decaying signal after a 90° pulse is called the free induction decay (FID); it has a decay constant mostly governed by T_2^*.

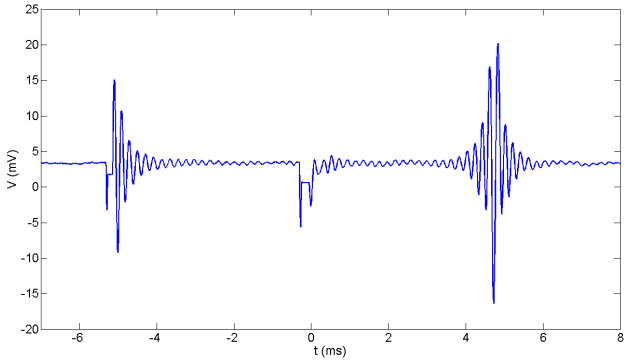

FIG. 1. A scope trace of the phase detector signal following a 90° – τ – 180° sequence on a 96% by weight glycerin sample. This trace is averaged over 16 readings, at τ = 5ms with a 100ms repeat time. Note the FID clipping after each pulse.

III. TECHNIQUES AND PROCEDURE

Before making any measurements, it is necessary to determine the durations corresponding to 90° and 180° pulses. We use the spin echo: when $\omega \approx \omega_0$, the echo amplitude is maximal following a 90° – τ – 180° pulse. Thus, we vary PW1 while setting PW2 to twice PW1. We look for values of PW1 which maximize the spin echo and take the highest of any indistinguishable values. PW1 is thus the duration of the 90° pulse, and PW2 the 180°

When doing this measurement, we typically use a τ and repeat time of approximately 5 ms and 100 ms, respectively. The the 90° pulse varies according to the nucleus and the RF amplitude; it also depends slightly on the probe orientation. Hence, we redetermine it each lab session and when switching to a different nucelus. We usually find between 10 and 20 µs for the proton.

We present the following procedures in order of complexity. Thus, we discuss the measurements of γ, T_2, and T_1, in that order.

III.1. Gyromagnetic Ratios

According to Equation 1, we can obtain γ from measuring B_0 and ω_0. We find ω_0 by noting that after a 90° pulse, the FID frequency is the difference $|\omega - \omega_0|$. Hence, we adjust the RF frequency ω to decrease the FID frequency to zero (the result is a critically damped FID). This condition means $\omega = \omega_0$, and we read off $\omega_0 = \omega$.

We measure $\omega_0 = (7.512 \pm 0.001)$MHz for the proton and $\omega_0 = (7.075 \pm 0.001)$MHz for the ^{19}Fl nucleus. The respective samples used are 100% glycerin by weight and a test tube labelled "fluoropolymers".

We also measure the field of the permanent magnets. Using an RFL Hall effect gaussmeter zeroed using calibration magnets, we find the field in the probe coils is $B_0 = (1730 \pm 10)$G for both cases.

Thus, we can calculate the gyromagnetic ratios of $\gamma = (2.728 \pm 0.016) \times 10^8\,\mathrm{s^{-1}T^{-1}}$ for the protons in glycerin, and $\gamma = (2.570 \pm 0.015) \times 10^8\,\mathrm{s^{-1}T^{-1}}$ for the ^{19}Fl nuclei in the fluoropolymer sample.

III.2. Spin-Spin Relaxation

We measure the spin-spin relaxation times using the spin echo technique described in [2]. As discussed in Section I, a spin echo occurs after a $90° - \tau - 180°$ sequence and directly measures T_2; the governing equation is

$$V(\tau) = V_0 e^{-2\tau/T_2} \tag{2}$$

where V_0 is the initial amplitude of the FID after the 90° pulse (or equivalently, the spin echo amplitude at $\tau \approx 0$), and $V(\tau)$ is the amplitude of the spin echo having waited a delay time τ before the application of the 180° pulse. For a sample of the output we expect, see Figure 1.

We measure the amplitude of the spin echo for approximately ten values of τ using the $90° - \tau - 180°$ method for each aqueous solution of glycerin, with samples labelled by percent weight. In this lab, we use the sample set $\{100\%, 98\%, 96\%, 95\%, 94\%, 92\%, 90\%, 84\%, 85\%, 70\%\}$. The ranges of τ used were 3–12 ms in steps of 1 ms for 100% down to 84%; 1–10 ms in steps of ms for 80%; and 5–55 ms in steps of 5 ms for 70%.

To eliminate the background noise and obtain better readings, we set the oscilloscope on averaging, with averaging values of either 8 or 16, depending on the sample. To determine the errors, we measure the maximum and minimum amplitude of the spin echo signal at $\tau = 5$ms as the signal fluctuates with averaging off. Thus, assuming a uniform distribution, the error bars on the data are this fluctuation divided by $\sqrt{12}$ and by the square root of the number of averagings. The data for the case of 96% glycerin is shown in Figure 2.

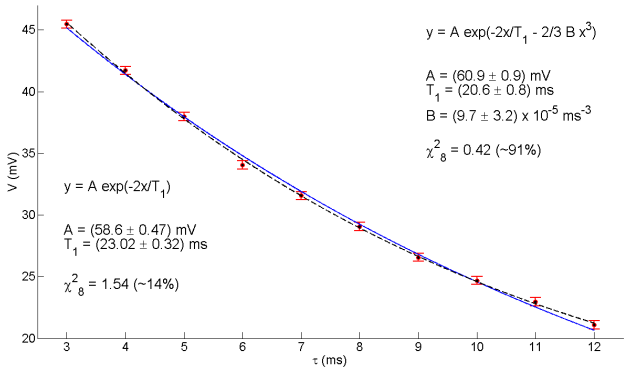

FIG. 2. V vs τ for 96% glycerin. The solid line (bottom left) is the fit according to Equation 2, while the dashed line (upper right) is the fit to Equation 4 (see Section IV.1).

III.3. Spin-Lattice Relaxation

We measure the spin-lattice relaxation times using the "three pulse sequence" described in [2], which consists of the sequence $180° - \tau - 90° - 180°$. The initial pulse inverts the spin population, causing the magnetization $\mathbf{M}$ to point in the $-\hat{\mathbf{z}}$ direction. During the time delay τ, the spins return to thermal equilibrium by giving off energy to the surrounding lattice, and $\mathbf{M}$ recovers its $+\hat{\mathbf{z}}$ component. Thus, the magnitude of $\mathbf{M}$ starts out large, crosses zero and then grows again. The governing equation is

$$\mathbf{M}(\tau) = M_0 \left(1 - 2e^{-\tau/T_1}\right) \hat{\mathbf{z}}$$

where $M_0 = |\mathbf{M}(\tau \approx 0)|$ is the magnitude of the intial magnetization. To actually find the magnetization, we use the 90° pulse to place $\mathbf{M}$ in the transverse plane; the intial amplitude $V(\tau)$ of the second FID is a measure of $M(\tau) = |\mathbf{M}(\tau)|$. If the sequence ended here, measurement of $V(\tau)$ is just the "population inversion method".

However, in the three pulse sequence, the pulse programmer waits a short amount of time ϵ (on the order of 1 ms; the exact value is not well documented) before applying a 180° pulse, with the goal of measuring $V(\tau)$ with a *spin echo*. The technique is motivated by the difficulty in measuring the initial amplitude of an FID—the circuitry clips about 1 ms of the signal after each pulse. Since ϵ is small compared to T_2 for a Fe^{3+} solution, we do not introduce any confounding spin-spin effects. Hence, measuring the amplitude of the spin echo effectively measures $V(\tau)$, and the expected model is, with $V_0 = V(0)$,

$$V(\tau) = V_0 \left|1 - 2e^{-\tau/T_2}\right| \tag{3}$$

We measure the spin echo amplitudes for about 10 values of τ for each sample of Fe^{3+} solution. The samples come from a serial dilution starting at 8.30×10^{-2} M for solution #1 and 1.66×10^{-2} M for solution #2; subsequent odd and even solutions are 1/10 the concentration of the preceding solution of the same parity. For this lab, we use the sample set $\{\#2, \#3, \#4, \#5, \#6\}$. The ranges of τ used were 2–7 ms in steps of 1 ms for #2; 2–12 ms in steps of 1ms for #3 and #4 (including 13ms for #4); 5–135 ms in steps of 10ms for #5; and 5–550 ms in steps of 50ms for #6.

As with T_2, we use averaging to reduce noise, and we measure error the same way. The raw voltage amplitude data for solution #5 is shown in Figure 3.

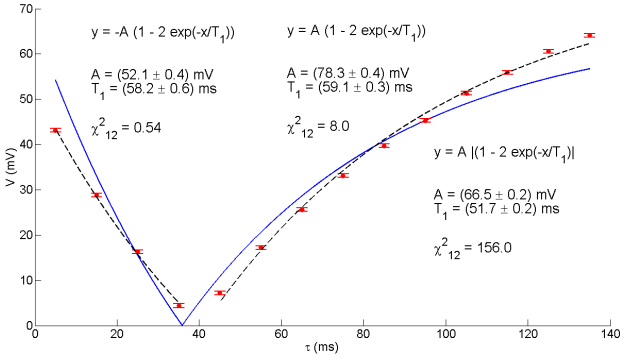

FIG. 3. V vs τ for Fe^{3+} solution #5. The solid line (bottom right) is the fit according to Equation 3, while the dashed line (upper left, right) is the fit to Equation 5 (see Section IV.2).

IV. ANALYSIS OF DATA

IV.1. Spin-Spin Relaxation

Using the table at [5], with an estimated room temperature of 20 °C, we can find the viscosity η of the glycerin samples. This allows us to determine the relationship between viscosity and T_2. These results are tabulated in Table I below.

However, for low viscosity, the spin echo technique for determining T_2 suffers from the effects of diffusion. If, during the delay τ, the components of the sample *diffuse* from one field strength to another, the result is a residual effect of the field inhomogeneity in spite of the spin echo approach. According to [2], considerations of diffusion changes Equation 2 to

$$V(\tau) = V_0 \exp\left(-\frac{2\tau}{T_2} - \frac{2}{3}\gamma^2 G^2 D\tau^3\right) \tag{4}$$

where G is the gradient of the inhomogeneous field and D the diffusion constant. This model predicts that when viscosity is low, the echo ampltitude V is further suppressed by a term exponential in τ^3.

Using this alternative model, we obtain another estimation T_2' of the spin-spin relaxation time, which are also presented in Table I. As expected, T_2' deviates more from T_2 for lower viscosities (and higher values of τ used), suggesting diffusion does affect the measured spin echo.

TABLE I. Estimations of T_2 for various glycerin samples.

% by Weight	η (cP)	T_2 (ms)	T_2'(ms)
100	1410	14.30 ± 0.26	13.57 ± 0.66
98	939	19.07 ± 0.50	18.1 ± 1.3
96	624	23.02 ± 0.32	20.58 ± 0.77
95	523	24.76 ± 0.50	21.5 ± 1.2
94	437	30.18 ± 0.43	27.7 ± 1.1
92	310	36.07 ± 0.92	31.3 ± 2.3
90	219	43.93 ± 0.10	41.05 ± 0.29
84	109	66.3 ± 2.5	52.5 ± 4.0
80	60.1	96.9 ± 4.3	141 ± 24
70	22.5	89.5 ± 1.2	100.6 ± 3.4

Finally, we combine the results of the two models by taking the error weighted average, and also use as our systematic error the difference between the two models. Following N. Bloembergen's thesis,[1] we plot these final values of T_2 against η in a log-log plot, observing a linear trend in the data. We fit a linear model $y = ax + b$ to the log-log data, and obtain the parameters $a = -0.49 \pm 0.03$ and $b = 2.75 \pm 0.08$ with a chi-squared value $\chi^2_8 = 1.29(24\%)$. This plot of the final results, along with the fit, is shown in Figure 4.

IV.2. Spin-Lattice Relaxation

Using the serial dilution, we know the concentration $[Fe^{3+}]$ of ions in the solutions. This allows us to determine the relationship between T_1 and paramagnetic ion concentration. The results are tabulated in Table II.

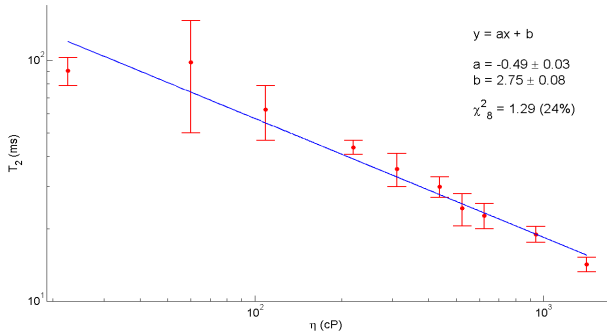

FIG. 4. Best estimates of T_2 vs η on log-log scale for samples of glycerin, with a linear fit to the data.

As apparent in Figure 3, however, there appears to be a systematic shift in the two different portions of the fit. To explore the implications, we introduce another model, splitting the data into two sets based on the τ_0 value of magnetization turning point.

$$V(\tau) = \begin{cases} -V_0\left(1 - 2e^{-\tau/T_2}\right) & \tau < \tau_0 \\ V_0\left(1 - 2e^{-\tau/T_2}\right) & \tau > \tau_0 \end{cases} \tag{5}$$

The estimations on T_1 given by the two pieces are averaged together and labelled T_1'. The results are also tabulated in Table II.

TABLE II. Estimations of T_1 for various paramagnetic ion samples. Note that no τ_0 was found for solution #2.

Solution No.	$[Fe^{3+}]$ (M)	T_1 (ms)	T_1'(ms)
2	0.0830	0.86 ± 0.02	—
3	0.0166	3.36 ± 0.01	3.47 ± 0.01
4	0.00830	5.57 ± 0.02	6.29 ± 0.03
5	0.00166	51.7 ± 0.6	59.0 ± 0.3
6	0.000830	347 ± 18	382 ± 7

We combine T_1 and T_1' in the same way as with T_2. However, plotting the results on a log-log plot is not particularly illuminating. The data is roughly linear, but the error bars appear to be heavily underestimated. The resolution of this problem remains difficult. The final results, as well as an attempted fit, is given in Figure 5.

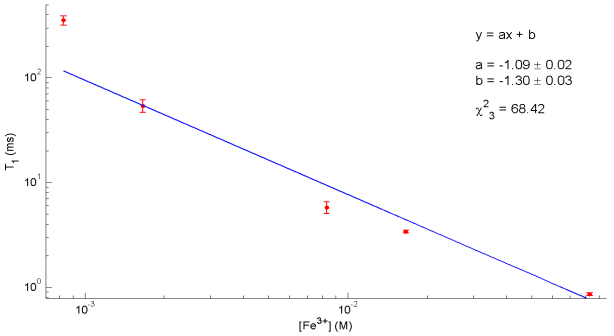

FIG. 5. Best estimates of T_1 vs $[Fe^{3+}]$ on log-log scale for Fe^{3+} solutions, with a linear fit to the data.

V. CONCLUSIONS

We determined the gyromagnetic ratios of the proton and ^{19}Fl nucleus to be $\gamma = (2.728 \pm 0.016) \times 10^8\,\mathrm{s^{-1}T^{-1}}$ and $\gamma = (2.570 \pm 0.015) \times 10^8\,\mathrm{s^{-1}T^{-1}}$. This is a fractional difference from published values of 2.17% and 1.98%, both overestimates. Interestingly, the discrepancy is very similar in both cases, and should be attributable to a systematic error in the determination of B_0.

Furthermore, we examined spin-spin relaxation in aqueous glycerin solutions and spin-lattice relaxation in paramagnetic ion solutions. We observed a trend in the data in log-log space, with a noticeably inverse linear relationship for glycerin, as claimed by N. Bloembergen. This suggests a power function dependence of relaxation on viscocity and concentration, the physical nature of which inspires investigation.

Most importantly, we confirm the use of spin echo techniques and pulsed NMR spectroscopy in general as a laboratory tool in exploring material properties.

[1] N. Bloembergen, *Nuclear Magnetic Relaxation: A Reprint Volume* (W.A. Benjamin, 1961).

[2] M.I.T. Junior Lab Staff, "Pulsed Nuclear Magnetic Resonance: Spin Echoes," (2011).

[3] R. Freeman, *A Handbook of Nuclear Magnetic Resonance* (Longman, Harlow, 1988).

[4] E. Hahn, Phys. Rev. **80**, 580 (1950).

[5] DOW Chemical Co., "OPTIM - Physical Properties - Viscosity," (2011).

ACKNOWLEDGMENTS

EN gratefully acknowledges his lab partner, Kevin Galiano, and the Junior Lab staff for their assistance in understanding the theory behind the design and analysis of this experiment.